

Bidirectional Electric Vehicle Based on off-board Charger Design

Adel A. Elbaset¹ and Shazly A. Mohamed^{2*}¹Department of Electromechanics Engineering, Faculty of Engineering, Heliopolis University, Cairo, Egypt²Department of Electrical Engineering, Faculty of Engineering, South Valley University, Qena, Egypt,*Corresponding author: Shazly A. Mohamed¹

Article history: Received: 02-05-2024 Revised: 30-05-2024 Accepted: 1-06-2024

Abstract

The continuity of the energy grid is the result of building a breed of ever-increasing demand for innovative electrocatalysis and the most effective solutions that qualifies the active sharing by end users in the balanced and trustworthy management of energy systems. One emerging prospect for such bidirectional exchange of electrical energy through the network and consumers is scope for the development of bidirectional energy trading among energy suppliers and owners of electric vehicle. It is proposed in this article to design a bidirectional, 3-phase, 2-stage off-board EV charger. The first step works as an AC/DC converter through the charging process, runs as 3-phase inverter and improves power factor while power is exchanged from the V2G. The next step is a DC/DC converter connected to first step via a DC-bus. A grid bypass filter is prepared to activate grid interconnection without noticeable problems in power quality. Suggested design and innovative infrastructure were examined during a simulation-based MATLAB software environment by connecting charger to a 3-phase micro-network and the results are consistent with the performance of suggested charging topology. Index Terms: Electric Vehicle (EV), Bidirectional Charger, Power Quality, Micro-grid, Vehicle-to-Grid (V2G)

1. Introduction

The increased international contact along with challenges such as depleting of traditional energy sources and environmental interests positively confirm researchers' insistence on innovating alternative energy economical and environmentally solutions. The emerging technological inventions in this regard, electric vehicle batteries are used as storage and support solution to improve the scenario of using different electrical energy by participating actively in responding to the demand either by reselling the stored energy or throttling the freight broker [1]. The idea of using high-density electric vehicle batteries as the source for injecting electrical energy into network has provided numerous advantages to electric vehicle owners, such as income generation and network congestion management through fill the valley and shave the peak, which means more renewable energy sources for energy production, and source of support in case of indigence or power outages, improving the reliability of microgrids while participating in virtual power plants. Nevertheless, regardless of these there are many advantages, the only obstacle is the resulting stresses in minimized lifespan of electric vehicle batteries because of overcharge and/or discharge cycles. Therefore, the application of V2G is still at the industrial level encounters lots of technology embarrassment which leaves room for new research and development.

The nagging concern about global warming and greenhouse gas emissions leads to many innovative & creative solutions in many parts of the life to embrace greener and more environmentally friendly lifestyle at the national and individual levels. It is mentioned that, there was a significant of 27% contribution to USA greenhouse gas emissions by transportation sector alone in 2020 [2] as shown in Fig. (1). Consequently, there is a clear global trend of shift towards more environmentally friendly

selections in all part, for example, in the transport sector, traditional fossil fuel-powered transport has been replaced, and the adaptation of electric vehicles can be a revolting step towards detergent ecology. The benefit is that the EV can be fueled from environmentally friendly renewable energy production sources, regardless of the traditional fuel sources. And then, energy storage infrastructure, for example: batteries and its charges, it is actively researched to enhance its efficiency. And there some still are critical issues with electric vehicles such as expensive batteries, life cycles restricted [3], additional cost, and PQ around electric vehicle chargers and inefficiency in electric vehicle charging circuits. Issues related to PQ active filters can be handled [4, 5].

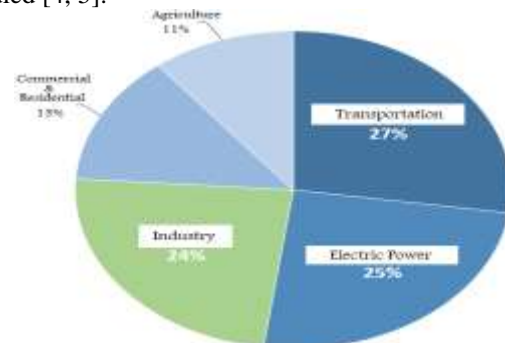


Fig. 1. Sources of emissions by sector as in [6]

The unidirectional on-board charger implemented at EVs is typically slightly of the vehicle itself and only allows EV battery to be charged through a unidirectional power flow from G2V. Despite a relatively new concept of the V2G process whereby a stored energy electric vehicle can export its energy to the grid, it guarantees many of the above benefits and is applicable where vehicle is parked 85% at that time. Depending on mounting site of an EV charger, two categories have been identified in literature:

(a) Chargers On-board are devices composite within EVs that operate on either 1-phase or 3-phase power supplies. Being portion of an EV increases its weight and size which impedes mobility in some way, so its power & size classification are restricted [7], [8].

(b) Chargers Off-board is devices mounted and combined into designated stations where the electric vehicle can connect battery extremes for charging. Since it does not affect the design of the electric vehicle, these kinds of chargers are commonly larger in size and high rated of power [9], [10].

The V2G process enables the bi-directional flow of energy and it allows energy exchange through the vehicle and the grid in any direction. V2G specifically refers to the real power flow from vehicle to grid, nevertheless, it can also provide reactive power reparations, and reactive energy flow is freelance for state of charge (SOC) of the battery. The main use for reactive energy support is, it can perform such as VAR reparations and minimize long-distance reactive energy transmission losses in the network by balancing the VAR load demand locally. Moreover, charging from renewables during activity hours, then feeding that energy through idle hours could be an effective solution to the interrupted problems of renewables. There are inherent limitations in the capacity of on-board chargers and an EV is effectively navigated via off-vehicle chargers because they have such high and stable strength rates that they can operate under an additional services agreement etc. [33]. A pivotal aspect of V2G application is to activate the communication among the network and the vehicle in order to interchange data, for example, operating mode, battery SOC etc. The communication standard IEC 61850 [11] specifies standards to be followed for the interchange of information among smart electronic devices within the substation whereas IEC 61850-7-420 [12] pilot schemes in the area of communication related infrastructure for renewable energy generation and IEC 61850-7-420 [13] has been extended to consider components that do not fall under the above criteria. Nevertheless, EVs operations and V2G remained unintergrated till IEC 61850-90-8 [14] was suggested to fit perfectly electric vehicles into smart grids. Desirable properties of an EV charger are high energy density and efficiency, bidirectional energy flow and low current ripple, etc [15, 16].

In [17] it was proposed that the problem of electricity shortage could be solved by establishing electric charging stations based on PV generators. Also San Diego elaborated this modification and designed first self-contained electric charging station based on solar energy. Nevertheless, the drawback of these strategies that's solar energy can be mainly obtainable from 8am to 5pm through the day which is the efficient timing to most jobs. To address it's a problem, [18] was suggested to design charging stations in the workplace where most people can charge their electric vehicles through working time. In [19] some techniques have been suggested to design a minor electric vehicle chassis to reduce electricity consumption. In [20] the subject of the electric vehicle charging has been countered by proposing some smart charging techniques.

Intelligent charging can work in unidirectional & bi-directional modes. For unidirectional mode, electric vehicles can be charged only as in G2V mode. For bi-

directional mode, energy can flow in V2G and G2V mode directions. The bi-directional type has more features because it's able to return energy to grid through peak hours. Electric vehicle charging can be assorted in two groups: centralization technique [21, 22] and decentralization technique [23-25]. In the centralization approach, charging of EV is determined by a collector and in the decentralization technique; the EV owner determines V2G or G2V mode.

In [26] various architecture of bidirectional with DC-DC Converter is illustrated. This configuration has the same function with the included DC-DC converter & bi-directional AC-DC converter. Control architecture applied in this model is accountable for maintaining the power factor one and ameliorates the energy quality. Nevertheless, problem with this architecture is that it can perform only a THD of 8%. More switches are included in this structure and that is the reason for the more loss of conductivity which is the main defect of this structure. In [27] it is recommended to reduce the THD of the 3-phase input, which is converted from the AC mains at a higher frequency and at the battery voltage level during the step-down converter. Then, this voltage is converted into direct current during the rectifier. As there are more switches, this structure fails to emerge again owing to increased conduction loss. This structure has lowered THD but the lower-order harmonics persisted.

In [28] another architecture was entered in which the AC-AC is converted during dual active bridge transformer [29] followed by a sequential buzz tank, step-down transformer and then through a 1-phase converter, this AC voltage is inverted or reversed depending on operation mode or current direction. The feature of this structure is to achieve more efficiency and soft transition phenomenon. Nevertheless, the drawback of this architecture is again more switches being shared and more delivery loss.

In [30] a 2-stage, 3-phase bi-directional charger for electric vehicles was proposed. First step is depending on AC-DC and next step is DC-DC converting. Moreover, charger is designed with not isolated transformer depend on half-bridge rectifier and an isolated transformer is depend on an active double-bridge rectifier. The drawback of the charger is only exchanges real energy, thus the electric vehicle can't be applied as fixed VAR compensator which is one of interests of the EVs.

There are two categories of electric vehicle chargers depending on where internal battery and external chargers are installed [31], [32]. On-board types are composite within EVs that operate on single or 3-phase power supplies. Off-board types are docked and combined at some stations where the electric vehicle can be connected battery extremes for charging. Since they do not influence the design of an electric vehicle, these kinds of chargers are commonly more powerful and larger in size.

This paper aims to design a bi-directional, 3-phase, 2-stage, off-board EV charger adequate for two modes G2V & V2G by allowing bi-directional energy exchange among the vehicle and grid. The proposed design was tested by integrating it with a 3-phase AC micro-grid consisting of a diesel generators set with renewable resources. For example, photovoltaic and wind generation units. The implementation of suggested design as well as its control

structure was simulated using MATLAB program to accurately test the results in V2G & G2V modes.

This research is structured as follows after introduction: firstly, in section (2) the methodology and modeling of the proposed work is described. Then, in Section (3), the system modeling and simulations with results of the proposed architecture is detailed and discussed. After that, Section (4) presents the results of simulations and comparison significantly. Finally, conclusions about the performance of the suggested structure are investigated in Section (5).

2. Proposed work modeling and approach

A 100KVA, 2-stage, 3-phase electric charger is designed for high-density electric vehicle batteries that support charging and dis-charging processes. The basic components of architecture design are: Micro-grid design, LCL filters, three-phase power factor improvement and bidirectional voltage converter as depicted in Fig. (2). Design and control formulation as well as parameter settings they are explained in the following branches.

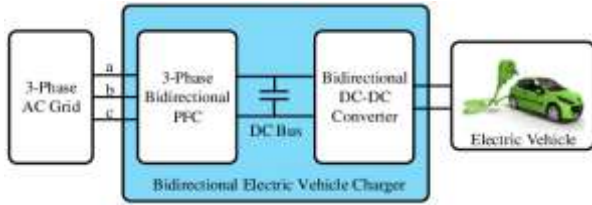


Fig. 2. A general bi-directional EV charger design block diagram

In G2V mode, the vehicle draws power from micro-grid and the battery is charged where the electric vehicles behave as a micro-grid load conventional. In spite of, during V2G mode, electric vehicle can insert its stored energy to micro-grid while the battery is being discharged. Three-phase rectifier step by charging mode operates as 3-phase stage controlled by inverter and a PFC-to-grid stage in V2G mode. Fig. (3) shows direction of current and energy flow for V2G & G2V operation modes.

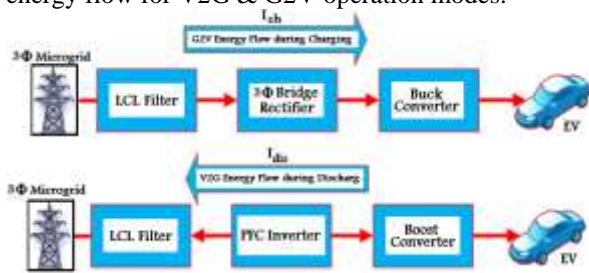


Fig. 3. Energy flow for V2G and G2V operation modes

2.1 Micro-grid Design Methodology

A micro-grid is an interconnected network of generating units and distributed loads which it can operate in two modes, For example, connected to grid and island. In networked mode, this grid is attached to the main network but operates separately in island mode. The main network usually composed of a central obstetrics unit, large transmission grid and can covering a wide area. Otherwise,

micro-grid includes the distribution of energy sources consisting mainly of distributed wind generators, PV generators, and sometimes, electric vehicles. In this article, this bi-directional charger of electric vehicle is designed so that it can operate in both modes G2V and V2G with charging and discharging modes respectively. The micro-grid is designed to connect many loads and generators were distributed across several nodes. And therefore, in order to characterize behaviors in real-time, loads and generators are randomly selected.

2.2 LCL filter-Grid side Mathematical Model

An LCL filter is applied on grid side to connect an EV charger to 3-phase network which has key interests for LCL such as, reducing harmonics of the switching frequency created in the next step of the circuit, fewer disturbances in sensitive loads, less loss and lower THD. Also, ensures energy quality injected to the network in V2G operating modes. The LCL filter capacitor exceeds high shunt harmonics and hence the inductor size required is reduced as well as better separation among the filter and network resistance since the LCL filter provides less current ripples through the existing grid [34, 35].

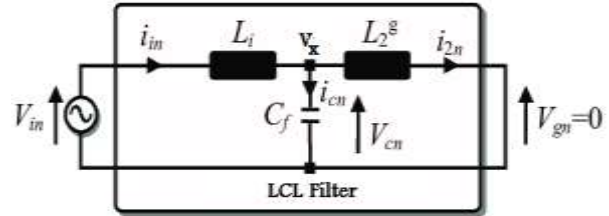


Fig. 4. Simple equivalent circuits for each stage with an LCL filter

Figure (4) shows the simple representation of the equivalent circuit for each stage using an n-harmonic LCL filter. Where, L_1 is the inductor of the converter side, L_2 is the inductor of the grid side; i_g or i_{2n} it is a pre-phase grid current and V_s or V_{in} it is a converter side voltage. For simplicity neglect the effect of the resistor [36]. The transfer function among grid current (i_g) and converter voltage (V_s) for the given circuit is expressed in Eq. (1).

$$\frac{i_g}{V_s} = \frac{1}{j\omega L_2 + j\omega L_1 - j\omega^3 L_1 L_2 C} \quad (1)$$

2.2.1 The selected parameter for the inductors

Addressing the transfer function in equation (1) gives us the determination of the values of the filter inductances.

$$|L| = \left| \frac{1}{\omega_{sw} \left\{ \frac{i_g(sw)}{V_i(sw)} \left(1 - \frac{\omega_{sw}^2}{\omega_{res}^2} \right) \right\}} \right| \quad (2)$$

Where, $L = L_1 + L_2$, $i_g(sw)$ is the current in frequency switching, $V_i(sw)$ is the input voltage when frequency switching, ω_{sw} is switching frequency and ω_{res} is resonance frequency $\frac{1}{\sqrt{CL_f}}$, and

$$L_f = \frac{L_1 L_2}{L_1 + L_2} \quad (3)$$

Where, L_1 is the inductor of the converter side and L_2 is the inductor of the inverter side [37]. As per IEEE standard. $i_g(sw) = 0.3\%$ of i_g , $V_i(sw) = 0.9\%$ of V_i , V_L is the voltage across the inductor, for example: $V_L = 0.2 * V_g$ for L_{max} , where $L_{max}/2 = L_1 = L_2$. Therefore, two inductors of equal value are used in the LCL filter [38].

2.2.2 The capacitor selected parameter

The capacitor value is determined depend on the famous consideration which the reactive power requirement of the capacitor should be restricted to 5% of rated power [39].

$$Q_c = 5\% \text{ of } S_{rated} \tag{4}$$

$$Q_c = \frac{V^2}{0.5 \pi f c} = 5\% \text{ of } S_{rated} \tag{5}$$

$$C = \frac{(0.05)S_{rated}}{2 \pi f V_g^2} \tag{6}$$

Where, S_{rated} is the rating of apparent power, Q_c is the capacitor reactive power, C is capacitor value, V is voltage and V_g is pre-phase grid voltage. As obvious, capacitor value depends on the frequency i.e., f_{res} , f_{sw} This finally depends on device limitations, size, cost, heat capacities, etc.

2.3 Three stages to enhance power factor

The PFC stage composed of a 3-phase rectifier/inverter which is a two-way bridge it consists of six electronic power switches it is controlled by voltage and current control devices which are depend on a Park-Clark shunt combined with a phase-locked loop at feedback in order to guarantee operation at unit power factor. Fig. (5) shows the schematic circuit for a 3-phase PFC.

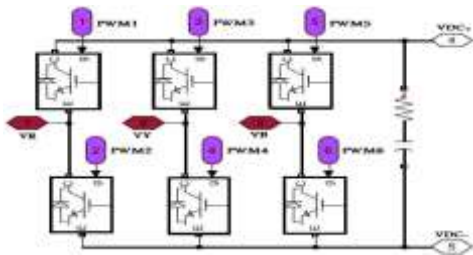


Fig. 5. Schematic Diagram of a 3-phase PFC stage

The PWM control mechanism applied to control the PFC phase switching is illustrated below that maintains a constant 800V DC in the DC-bus of PFC. Let a 3-phase measured voltage on grid side be:

$$V_g = [V_R \quad V_Y \quad V_B] \tag{7}$$

These voltages are converted to the field of $\alpha\beta$ and d_{qo} respectively through a coordinate transformation. After applying it, the $\alpha\beta$ transformation obtains two-dimensional parameters whereas zero in the third dimension.

$$V_a = [V_\alpha \quad V_\beta] \tag{8}$$

These parameters are fed to closed-loop controller as an input. The controller creates phase-angle (ωt) and also feedbacks it. The work of a conventional PLL is depicted in Fig. (6).

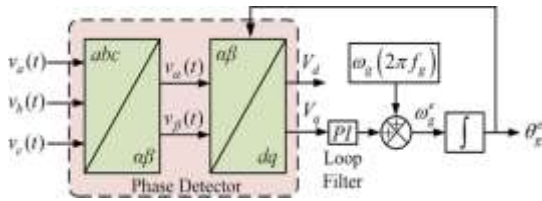


Fig.6. Schematic diagram for initial working of PLL

Likewise, the unfiltered 3-phase current LCL filter output I_{abc} is converted to field $\alpha\beta$ and then d_{qo} using the

PLL (ωt) output. The currents generated by I_d and I_q are applied to calculate the error regarding I_{dref} and I_{qref} which in part is fed to the PI controllers. The output voltage after adding appropriate duty gain is comparable to the carrier amplitude which is converted back to the 3-phase parameters of the reference voltage during reverse coordinate conversion. A reference voltage standard is applied as inputs to produce a PWM that finally controls the DC/AC conversion through the mode of V2G mode and conversely [40].

2.4 Bi-directional stage voltage level converter

This part composed of bi-directional a buck or boost converter and operates as a buck converter while in G2V mode, the charger is applied as boost converter. Polarity of the current signal determines charge and discharge process as it converts direction of the energy flows. PWM1 dominates top switch that performs buck operation whereas PWM2 dominates bottom switch corresponding to the boost operation.

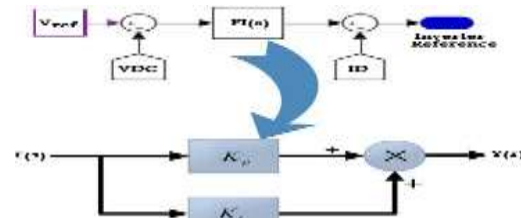


Fig.7. Diagram representation of the internal PI function

From Fig. (7), the transfer function of the PI controller includes proportional and integral coefficients K_p and K_i which leads to the output relationship given in equation (9):

$$Y(s) = E(s) * \left(K_p + \frac{K_i}{s} \right) \tag{9}$$

The basic layout of 3-phase inverters connected to grid is depicted in Fig. (8). Constant battery voltage is taken as input as the inverter is designed with BJTs and MOSFETS. The AC output is associated of this inverter to already introduced LCL filter, and then the 3-phase LCL filter output is associated to the network. For controller design, the 3-phase voltage is converted to 2-phases V_α and V_β by shifting parks. Then the PLL is implemented by these two voltages. Then V_α and V_β are converted into E_d and E_q via Clark's shift. Otherwise, all the 3-phase currents are transformed into I_α , I_β and then convert it as well to I_d and I_q with parks and Clark's shifts. And then, they are converted E_d , E_q , I_d and I_q are applied to generate six PWMs of inverter BJTs/MOSFETS in order to synchronize frequency, voltage, and sine waveform with a micro-grid.

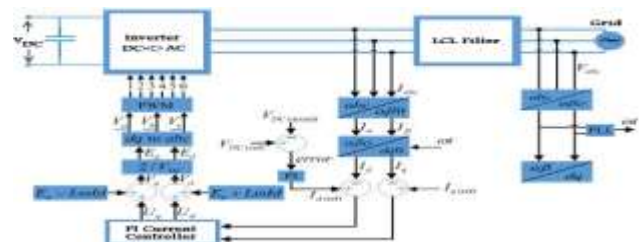


Fig.8. Schematic diagram for controlling a 3-phase PWM inverter

I_{ref} it is the current that shows converter behavior. Positive I_{ref} switches converter behavior to charging /G2V mode while negative I_{ref} indicates that, the converter operates in discharging & V2G mode as shown in Fig. (9).

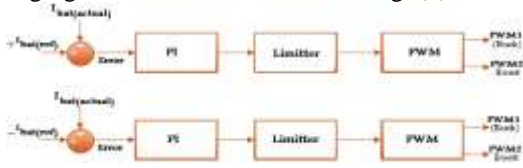


Fig.9. Battery charging and discharging diagram

2.5 Electric Vehicle Battery Specifications

Table (I) below shows the battery specifications selected for system modeling.

Table 1: System battery characteristics

Parameters	Values
Battery voltage nominal	350 V
Rated capacity of the battery	300 Ah
Initial charge State (%)	50 %
Response time of the battery	1s
Kind of battery	Sodium-ion
Cut-off voltage	260 V
Charged voltage completely	420 V
Nominal voltage capacity	270 V
Discharge current	130 A
Interior Resistance (Ω)	0.015 Ω

3. System Modeling and Simulations with Results

This section illustrates simulations and results for the suggested bidirectional charger EV and its impacts on the micro-grid where simulations were well-done on MATLAB R2020a software. So, for this purpose, a micro-grid has been designed that encompass some island-mode distributed generators such as: Photovoltaic generator, wind generator, diesel generator and the main utility network for grid-connected mode as depicts in Fig. (10). the major grid is applied 2500MVA/132KV.

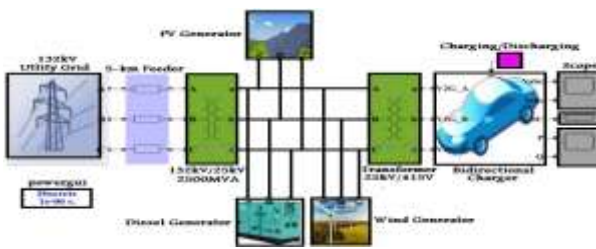


Fig.10. Complete studied system with Simulation

3.1 Main Utility Grid

A 2500MVA/120KV 3-phase voltage supply with frequency of 50Hz is modeled and designed to work as mains. Then with Star/Delta conversion, an 11KV/132KV step-up transformer is applied before transmission to decrease I^2R losses. Earthing transformer is utilized to preserve power grid from fault. Then, a 14-km long transmission line will be applied to transport electricity from main network to the distribution grid.

3.2 Photovoltaic Generator

The 12kW PV generator was designed in MATLAB software and 66 PV solar panel arrays that take radiation

and temperature as inputs and output to which DC power are applied. All PV modeling parameters are depicting in Table (II). Moreover, a boost converter is applied to increase the voltage into 500 VDC. This DC voltage is then transformed to 3-phase AC voltage with a three-level bridge inverter and further steps up to 25 kV with 3-phase delta/star transformers.

MPPT system for PV generator is applied with incremental conductance technique for maximum power. MPP is acquired when $\frac{dI}{dV} = 0$ where $P = V * I$.

$$\frac{d(VI)}{dV} = I + V \frac{dI}{dV} = 0, \quad \frac{dI}{dV} = -\frac{I}{V} \quad (10)$$

Where dI & dV are the principal components of the measured voltage and current ripples by the sliding time window T_{MPPT} .

Table II: PV modeling parameters

Parameters	Values
Parallel Strings of PV modules	66
Series connected unit	5
Cells/unit	96
Power (max) /unit	305W
Open-circuit voltage	64.5V
Voltage at P_{max}	53.8V
V_{oc} Temperature Coefficient	-0.28%
Short circuit current	6 A
Current at P_{max}	5.4 A
I_{sc} Temperature Coefficient	0.06 %
Cell Temperature	[0 25 50]
Series and Shunt resistances of the cell	$R_s=0.4 \Omega$, R_{sh} 269.5 Ω
Diode ideality factor	0.93

3.3 Wind Generator

The 50KVA/400V MATLAB Simulink wind generator is designed to maintain wind behavior. The wind induction block takes two inputs of wind, trip and providing 3-phase AC at the applied output. The trip is a binary entry that uses one to turn-off and zero is applied to turn-on the wind generator. The next entry called wind is applied to supply the transfer curve for the wind generator. This three-phase AC is boosted up to 25KV with delta/star conversion. All parameter values applied in modeling wind generators are shown in Table (III).

Table III: Wind generator modeling Parameters

Parameters	Values
Active power	50*10 ³ W
Line voltage	400V
Stator & Rotor resistances	$R_s=0.0045$, $R_r=0.0044$ pu
Stator & Rotor inductances	$L_s=0.125$, $L_r=0.18$ pu
Magnetizing inductance	$L_m=6.8$ pu
Inertia constant	5.1s
Coefficient of friction	0.01 pu
Nominal mechanical output capacity WT	12*10 ³ W
Base wind speed	12 m/s
P_{max} at base wind speed	1 pu
Proportional and Integral gains	$K_p=2$, $K_i=25$
Pitch angle in deg. (max)	45
Change maximum rate of pitch angle	2 deg./s

3.4 Diesel Generators

Simulink 15MVA/ 25KV model diesel generator also is applied as DG and synchronous devices block that takes two inputs, one to connect main actuator to excitation and the other to mechanical input. The Diesel generator generates 3-phase AC output which passes during a ratio of 1:1 isolation transformer and it is applied for safety purposes. 3-phase AC outlets are connected to the mains on the main model. The main drive/actuator system is carried out with control scheme by considering the mechanical energy.

3.5 Bi-directional Charger

The aim from this research is to design a 3-phase bi-directional EV charger, where the 3- phases input line from the main line is linked to an LCL filter. The inductor and capacitor values are computed using (2) and (4). After that, the LCL filter output is passed via 3-phase controllers that implement inverter or rectification operations as per requirement. Six PWMs are designed in order to control IGBT switching of a 3-phase controller. Then, a buck or boost process is accomplished on the DC voltage depend on charge or discharge operations. The 3-phase AC voltage is transformed to the DC via 3-phase rectifier and to charge the battery, DC voltage is reduced with buck converter in battery voltage levels. Whereas in V2G mode when vehicle energy is transported to the main grid, the battery DC voltage is augmented via the boost converter after that converted into a 3-phase AC with a 3-phase inverter. Moreover, the 3-phase voltage is override via the LCL filter and afterwards attached to network. The current and voltage are converted with a Clarks & Parks transform and a PLL is applied to secure it to the network.

Figure (11) shows the 3-phase voltages from the main carrier of all synchronous generating units, for example: utility grid, diesel, wind and photovoltaic generators in G2V mode. The results indicate that, all phase voltages are identical and exactly by 120 degrees.

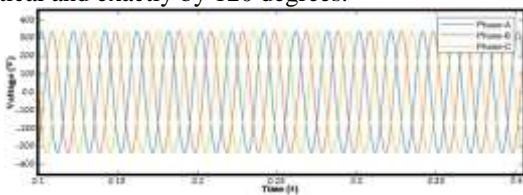


Fig.11. Three-phase voltages during G2V mode

Figure (12) shows the 3-phase current from main carrier of all synchronous generating units, for example: utility network, diesel, photovoltaic and wind generators in the G2V mode. The results indicate that, all phase currents are balanced by 120 degrees.

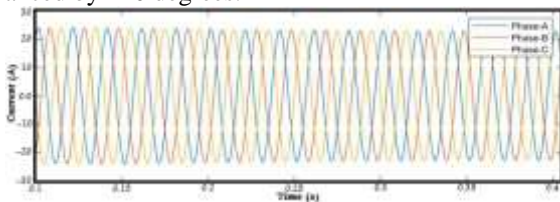


Fig.12. Three phase currents during G2V mode

Figure (13), shows the DC voltage in G2V mode before the converter and after rectification.

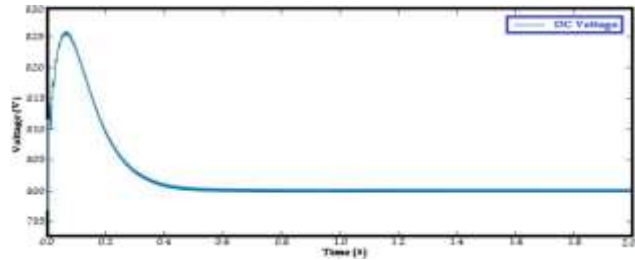


Fig.13. DC voltage in the G2V mode

Figure (14) shows the actual power consumed by a bi-directional charger while in G2V mode.

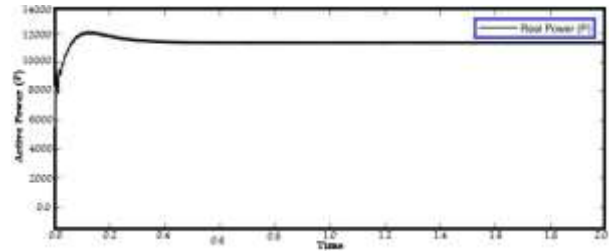


Fig.14. Active power consumption by bi-directional charger while in G2V mode

Figure (15) shows the consumed of reactive power by a bi-directional charger while in G2V mode.

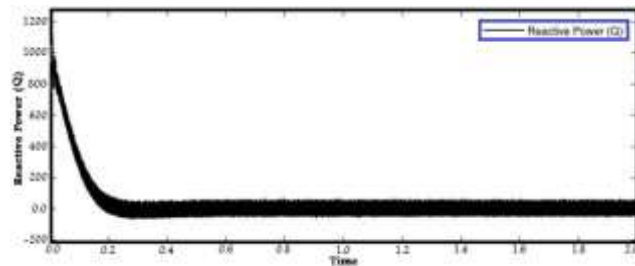


Fig.15. Reactive power consumption by bi-directional charger while in G2V mode

Figure (16) shows the 3-phase voltages from the main carrier of all synchronous generating units, for example: utility network, diesel, photovoltaic and wind generators in the V2G mode. The results indicate that, all phase voltages are identical and exactly by 120 degrees.

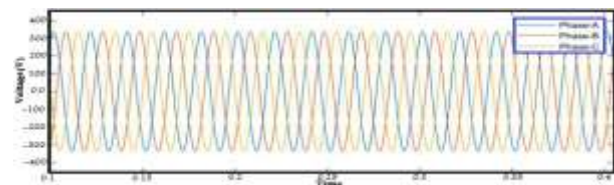


Fig.16. Three-phase voltages during V2G mode

Figure (17) shows the 3-phase current from main carrier of all synchronous generating units, for example: utility network, diesel, photovoltaic and wind generators in the V2G mode. The results show that, all phase currents are identical and completely balanced by 120 degrees.

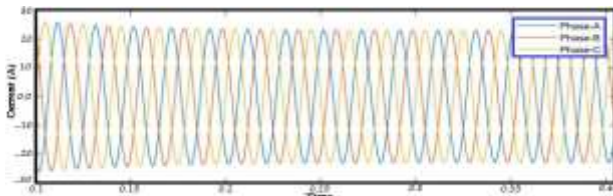


Fig.17. Three-phase Currents during V2G mode

Figure (18), shows the DC voltage of EV batteries in V2G mode after the converter and before 3-phase inverter.

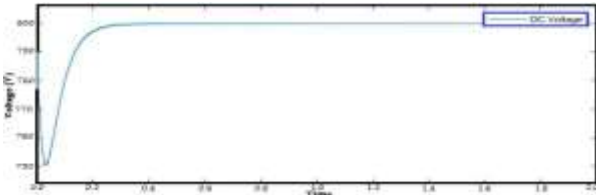


Fig.18. The DC Voltage in V2G mode after converter and before 3- phase inverter

Figure (19) shows the actual power provided by a bi-directional charger while in V2G mode.

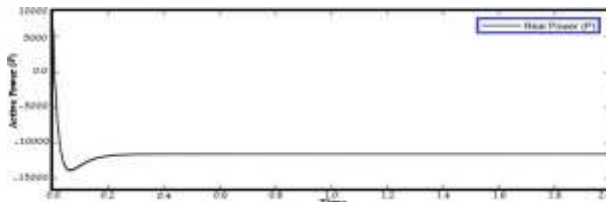


Fig.19. Active power supplied by bi-directional charger while in the V2G mode

Figure (20) shows reactive power provided by a bi-directional charger while in V2G mode.

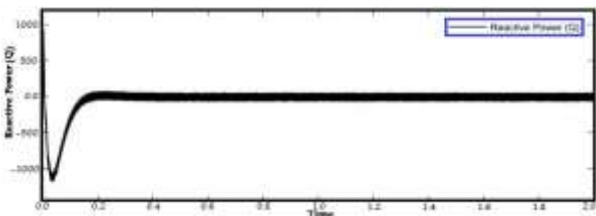


Fig.20. Reactive power is provided by bi-directional charger while in V2G mode

4. Compare and discuss results

The micro-grid is devised so that several generators are designed such as: PV, wind and diesel generators. By maintaining the same sequence all three of frequency, voltage and phase are in synchronized for optimal load management. After that, during the step-down transformer, the voltage drops to the secondary distribution level. The waveforms of voltage and current are shown in the simulation results. EVs batteries are inserted at secondary distribution level in either mode G2V or V2G. DC voltage after a 3-phase converter in G2V mode is shown in the same drawing. In Fig. (14), positive active power indicates that, real current is in the forward direction and the electric vehicle is taking power from network.

4.1 DC charging voltage comparison

It can be seen that, from Fig. (21), owing to the switching and charging devices, it takes more than 1s to reach the steady state for DC charging voltage. Despite this, in suggested scheme of Fig. (22) we can see that, steady-state is carried out in less than 0.12s.

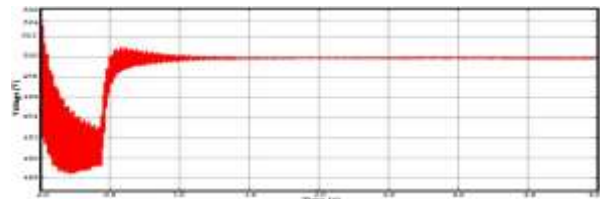


Fig.21. DC-link charging voltage is in G2V mode

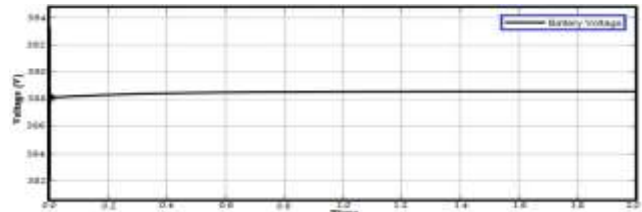


Fig.22. Battery voltage during G2V mode

4.2 Reactive Powers Comparison

In Figure (23), the reactive power is zero at all time and cannot be utilized as fixed VAR unless the proposed bi-directional EV charger can be applied as fixed VAR equivalent as shown in Figure (24).



Fig.23. Active and reactive energy discharge in G2V mode

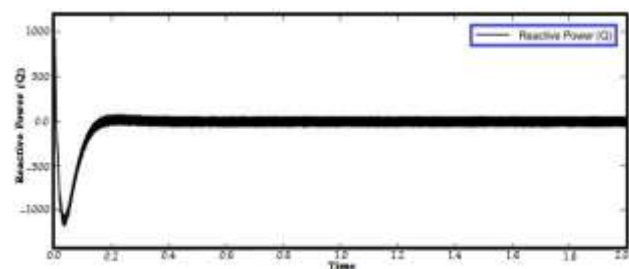


Fig.24. Reactive power is provided via bi-directional charger in V2G mode

4.3 Discharge voltages comparison

It is clear that, from Fig. (25), because devices are switched and charged, it takes more than 1s to attain the steady state discharging voltage. Despite this, in the suggested scheme of Fig. (26), we can see that, steady-state is carried out in less than 0.12s.

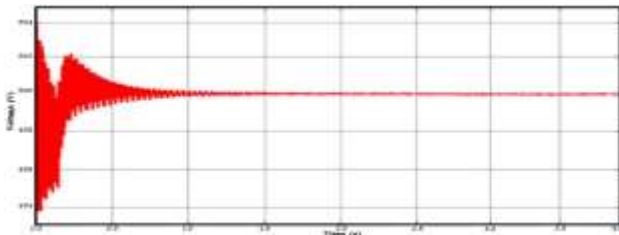


Fig.25. DC-link voltage not charging in V2G mode

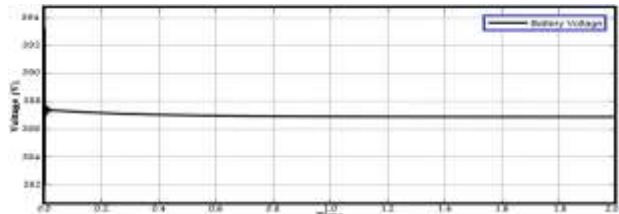


Fig.26. Battery voltage in V2G dis-charging mode

A graph with a negative value of true power denotes that, the current flows in opposite direction and the energy is the EV that supplies power to the network. All results are presented quantitatively; prove that bi-directional charger has capability to implement both V2G & G2V modes efficiently. So, the proposed system is much better than the latest systems regarding performance and concerns about power quality because the EVs batteries are among more expensive items and with ameliorative power quality the lifespan is increased. The following Table (IV) shows highlight comparison results:

Table IV: Contributions and Comparison with latest technique

Parameters	Reference [30]	Proposed System
Real power flow in forward and reverse	Yes	Yes
Reactive power flow in forward and reverse	No	Yes
Time to get a steady state	1.4s	0.04s
The transients	-2.6% - 1.2%	-0.2% - 0.06%

5. Conclusions

A bi-directional off-board EV charger has been introduced in 3-phase, 2-stages. The first step corrects 3-phase grid voltage to charge the targets while the subsequent step reduces the DC bus voltage to an appropriate level value for charging the battery and conversely. Enhancement of power factor allows the true and reactive powers to be exchanged of among two entities. LCL filters operates completely on the grid side to remain THD of the grid current within enveloped range about 5%. DC-link voltage still stable for each operating scenarios and there is no surge/skip whereas switching among modes or until the mains side voltage is deranged in some way. Results of a detailed systematic evaluation of charging and discharging patterns to verify robustness, controlling the suggested design, and to prove feasibility of its practical application.

Works Cited

[1] A. Y. Saber and G. k. Venayagamoorthy, "One million plug-in electric vehicles on the road by 2015" 12th International IEEE Conference on Intelligent Transportation Systems, St. Louis, MO, USA, pp. 141-147, 4-7 Oct 2009. DOI: [10.1109/ITSC.2009.5309691](https://doi.org/10.1109/ITSC.2009.5309691)

[2] M. Weiss, A. Zerfass, E. Helmers, "Fully electric and plug-in hybrid cars - An analysis of learning rates, user costs, and costs for mitigating CO2 and air pollutant emissions", Journal of Cleaner Production, 212 (2019), pp. 1478-1489, DOI: [10.1016/j.jclepro.2018.12.019](https://doi.org/10.1016/j.jclepro.2018.12.019)

[3] Shazly A. Mohamed, "Multi input rectifier stage for a system of hybrid PV/wind driven PMSG", SN Applied Sciences Journal, Vol. (1), No. (1578), pp. 1-18, November 2019. DOI: [10.1007/s42452-019-1629-3](https://doi.org/10.1007/s42452-019-1629-3)

[4] Shazly A. Mohamed, "Enhancement of Power Quality for Load Compensation Using Three Different FACTS Devices Based on Optimized Technique", International Transactions on Electrical Energy Systems, Paper 1-25, Dec. 2019. DOI: [10.1002/2050-7038.12196](https://doi.org/10.1002/2050-7038.12196)

[5] S. M. Jose, et al., "Multi-Phase Interleaved AC-DC Step-Down Converter with Power Factor Improvement", Micromachines (Basel), Vol. (14), No. (3): pp. 1-16, Mar. 2023, DOI: [10.3390/mi14030511](https://doi.org/10.3390/mi14030511)

[6] Soong-Ki Kim et al., "Widespread irreversible changes in surface temperature and precipitation in response to CO₂ forcing", Nature Climate Change, Vol. (12), pp. 834-840, Sept. 2022. DOI: [10.1038/s41558-022-01452](https://doi.org/10.1038/s41558-022-01452)

[7] G. Anjinappa, D. B. Prabhakar and W. Lai, "Bidirectional Converter for Plug-In Hybrid Electric Vehicle On-Board Battery Chargers with Hybrid Technique", World Electric Vehicle Journal, Vol. (13), pp. 1-16, Oct. 2022. DOI: [10.3390/wevj13110196](https://doi.org/10.3390/wevj13110196)

[8] K. Verma, M. Srivastava, P. S. Tomar, N. Sandeep and A. K. Verma, "Single-phase integrated converter with universal battery charging capability for plugin electric vehicles", IET Power Electronics Journal, Vol. (13), No. (4), pp. 821-829, 2020. DOI: [10.1049/iet-pel.2019.0847](https://doi.org/10.1049/iet-pel.2019.0847)

[9] Y. Lan et al, "Switched Reluctance Motors and Drive Systems for Electric Vehicle Powertrains: State of the Art Analysis and Future Trends", Energies Journal, Vol. (14), No. (8), pp. 1-29, Apr. 2021. DOI: [10.3390/en14082079](https://doi.org/10.3390/en14082079)

[10] M. Eull, L. Zhou, M. Jahnes and M. Preindl, "Bidirectional Nonisolated Fast Charger Integrated in the Electric Vehicle Traction Drivetrain", IEEE Transactions on Transportation Electrification Journal, Vol. (8), No. (1), pp. 180 -195, March 2022. DOI: [10.1109/TTE.2021.3124936](https://doi.org/10.1109/TTE.2021.3124936)

[11] A. Sachan, "Micro-grid: Low Power Network Topology and Control", International Journal of Electrical and Computer Engineering, Vol. (7), No. (12), pp. 1753 - 1758, 2013. DOI: [10.1307-6892/9997171](https://doi.org/10.1307-6892/9997171)

[12] D. Yadav, "Application of IEC 61850 standard to the integration of DER with the electricity network", IET Open Access Proc. Journal, Vol. (20), No. (1), pp. 696 -698, Sept. 2020. DOI: [10.1049/oap-cired.2021.0196](https://doi.org/10.1049/oap-cired.2021.0196)

[13] M. M. Esfahani and O. Mohammed, "An intelligent protection scheme to deal with extreme fault currents in smart power systems", International Journal of Electrical Power & Energy Systems, Vol. (115), No. (1), pp. 1-29, Feb. 2020. DOI: [10.1016/j.ijepes.2019.105434](https://doi.org/10.1016/j.ijepes.2019.105434)

- [14] T. S. Ustun, S. M. Hussain, M. H. Syed and D. Paulius, "IEC-61850-Based Communication for Integrated EV Management in Power Systems with Renewable Penetration", *Energies Journal*, Vol. (14), pp. 1-15, April 2021. DOI: [10.3390/en14092493](https://doi.org/10.3390/en14092493)
- [15] P. Singh, D. Yadav, S. Pandian, "5- Link between air pollution and global climate change", *Global Climate Change*, Vol. (14), pp. 79-108, March 2021. DOI: [10.1016/B978-0-12-822928-6.00009-5](https://doi.org/10.1016/B978-0-12-822928-6.00009-5)
- [16] J. Hansen and M. Sato, "Regional climate change and national responsibilities", *Environ. Res. Lett.*, Vol. (11), pp. 1-10, March 2016. DOI: [10.1088/1748-9326/11/3/034009](https://doi.org/10.1088/1748-9326/11/3/034009)
- [17] T. S. Biya, M. R. Sindhu, "Design and Power Management of Solar Powered Electric Vehicle Charging Station with Energy Storage System", 3rd IEEE International conference on Electronics, Communication and Aerospace Technology (ICECA), June 2019. DOI: [10.1109/ICECA.2019.8821896](https://doi.org/10.1109/ICECA.2019.8821896)
- [18] R. Dhawan, S. Karthikeyan, "An Efficient EV Fleet Management For Charging At Workplace Using Solar Energy", IEEE National Power Engineering Conference (NPEC), Mar. 2018. DOI: [10.1109/NPEC.2018.8476746](https://doi.org/10.1109/NPEC.2018.8476746)
- [19] S. Agrawal, S. Peeta, and M. Miralinaghi, "Multiparadigm Modeling Framework to Evaluate the Impacts of Travel Patterns on Electric Vehicle Battery Lifespan", *Journal of Advanced Transportation*, Vol. (2023), Article ID 1689075, pp. 1-12, Feb. 2023. DOI: [10.1155/2023/1689075](https://doi.org/10.1155/2023/1689075)
- [20] Pablo Luque et al., "Multi-Objective Evolutionary Design of an Electric Vehicle Chassis", *Sensors* 2020, pp. 1-22, Vol. (20), June 2020. DOI: [10.3390/s20133633](https://doi.org/10.3390/s20133633)
- [21] J. Yusuf, A. J. Hasan, L. F. Enriquez., and S. Ula, "A Centralized Optimization Approach for Bidirectional PEV Impacts Analysis in a Commercial Building-Integrated Micro-grid", *Electrical Engineering and Systems Science* pp. 1-38, April 2021. DOI: [10.48550/arXiv.2104.03498](https://doi.org/10.48550/arXiv.2104.03498)
- [22] M. Ntombela, K. Musasa, and K. Moloi, "A Comprehensive Review of the Incorporation of Electric Vehicles and Renewable Energy Distributed Generation Regarding Smart Grids", *World Electric Vehicle Journal*, Vol. (14), No. (176), pp. 1-28, July 2023. DOI: [10.3390/wevj14070176](https://doi.org/10.3390/wevj14070176)
- [23] J. Liao, H. Huang, H. Yang, and D. Li, "Decentralized V2G/G2V Scheduling of EV Charging Stations by Considering the Conversion Efficiency of Bidirectional Chargers", *Energies Journal*, Vol. (14), No. (4), pp. 1-16, Feb. 2021. DOI: [10.3390/en14040962](https://doi.org/10.3390/en14040962)
- [24] Shazly Abdo Mohamed and Abdel-Moamen M. A., "Design of a Low-cost PV Tracking System with Inverter", *Proceedings of 3rd International Conference on Energy Engineering*, Faculty of Energy engineering, Aswan University, Aswan, Egypt, Dec. 28-30, 2015.
- [25] F. Mohammadi, G. Nazri and M. Saif, "A Bidirectional Power Charging Control Strategy for Plug-in Hybrid Electric Vehicles", *Sustainability Journal*, Vol. (11), pp. 1-24, August 2019. DOI: [10.3390/su11164317](https://doi.org/10.3390/su11164317)
- [26] M. Coppola, P. Guerriero, A. Dannier, S. Daliento and A. Pizzo, "Inverter Operation Mode of a Photovoltaic Cascaded H Bridge Battery Charger", *Energies Journal*, Vol. (16), No. (13), pp. 1-5, June 2023. DOI: [10.3390/en16134972](https://doi.org/10.3390/en16134972)
- [27] J. Lozano, M. Montero, M. Guerrero, E. Cadaval, "Three-phase bidirectional battery charger for smart electric vehicles", 7th International Conference-Workshop Compatibility and Power Electronics (CPE), Tallinn, Estonia, June 2011. DOI: [10.1109/CPE.2011.5942263](https://doi.org/10.1109/CPE.2011.5942263)
- [28] S. Adhikary, P.K. Biswas, C. Sain et al., "Bidirectional converter based on G2V and V2G operation with time of usage-based tariff analysis and monitoring of charging parameters using IoT", *Energy Reports*, Vol. (8), pp. 5404-5419, May 2023. DOI: [10.1016/j.egy.2023.04.358](https://doi.org/10.1016/j.egy.2023.04.358)
- [29] Y. Wang, F. Ni, T. Lee, "Hybrid Modulation of Bidirectional Three-Phase Dual-Active-Bridge DC Converters for Electric Vehicles", *Energies Journal*, Vol. (9), No. (7), pp. 1-13, June 2016. DOI: [10.3390/en9070492](https://doi.org/10.3390/en9070492)
- [30] A. Tavakoli, S.Saha, M. Arif, M. Haque, N. Mendis, and A. M. Ool, "Impacts of grid integration of solar PV and electric vehicle on grid stability, power quality and energy economics: a review", *IET Energy Systems Integration Journal*, pp. 1-18, Dec. 2019. DOI: [10.1049/iet-esi.2019.0047](https://doi.org/10.1049/iet-esi.2019.0047)
- [31] N. Wong, and M. Kazerani, "A review of bidirectional on-board charger topologies for plugin vehicles", 25th IEEE Canadian Conference on Electrical and Computer Engineering (CCECE), Montreal, QC, Canada, Oct. 2012. DOI: [10.1109/CCECE.2012.6334957](https://doi.org/10.1109/CCECE.2012.6334957)
- [32] M. Kesler, M. C. Kisacikoglu, L. M. Tolbert, "Vehicle-to-grid reactive power operation using plugin electric vehicle bidirectional off board charger", *IEEE Transactions on Industrial Electronics Journal*, pp. 6778-6784, Vol. (61), No. (12), Dec. 2014. DOI: [10.1109/TIE.2014.2314065](https://doi.org/10.1109/TIE.2014.2314065)
- [33] J. Yong, R. K. Vigna, K. M. Tan, N. Mithulananthan, "A review on the state-of-the-art technologies of electric vehicle, its impacts and prospects", *Renewable and Sustainable Energy Reviews Journal*, pp. 365-385, Vol. (49), Issue (c), Sept. 2015. DOI: [10.1016/j.rser.2015.04.130](https://doi.org/10.1016/j.rser.2015.04.130)
- [34] D. Cittanti, F. Mandrile and R. Bojoi, "Optimal design of grid-side LCL filters for electric vehicle ultra-fast battery chargers", 55th IEEE International Universities Power Engineering Conference (UPEC), Turin, Italy, Sept. 2020. DOI: [10.1109/UPEC49904.2020.9209771](https://doi.org/10.1109/UPEC49904.2020.9209771)
- [35] Yong-Jung Kim and Hyosung Kim, "Optimal design of LCL filter in grid-connected inverters", *IET Power Electronics*, Vol. (12), Issue (7), pp. 1774-1782, June 2019. DOI: [10.1049/iet-pel.2018.5518](https://doi.org/10.1049/iet-pel.2018.5518)
- [36] C. Mahamat, M. Petit, F. Costa, R. Marouani and A. Mami, "Optimized Design of an LCL Filter for Grid Connected Photovoltaic System and Analysis of the Impact of Neighbors' Consumption on the System", *Journal of Electrical Systems*, Vol. (13), No. (4), pp. 618-632, Oct. 2017. DOI: <https://hal.science/hal-01676019>
- [37] D. Pan, X. Ruan, X. Wang, H. Yu and Z. Xing, "Analysis and Design of Current Control Schemes for LCL-Type Grid-Connected Inverter Based on a General Mathematical Model", *IEEE Transactions on Power Electronics*, Vol. (32), Issue (6), Jan. 2016. DOI: [10.1109/TPEL.2016.2602219](https://doi.org/10.1109/TPEL.2016.2602219)
- [38] S. Albatran, A. Koran, I. Smadi, and H. J. Ahmad, "Optimal design of passive RC-damped LCL filter for grid-connected voltage source inverters", *Electrical Engineering*

Journal, Vol. (100), No. (1), pp. 2499-2508, Dec. 2018.

DOI: [10.1007/s00202-018-0725-5](https://doi.org/10.1007/s00202-018-0725-5)

[39] Shazly A. Mohamed, "Design, Control and Performance Analysis of a Grid-Connected Hybrid System", the Egyptian International Journal of Engineering Sciences and Technology, Vol. (24), pp. 18–26, January 2018. DOI: [10.21608/eijest.2018.97217](https://doi.org/10.21608/eijest.2018.97217)

[40] S. Singirikonda et al., "Adaptive control-based Isolated bi-directional converter for G2V& V2G charging with integration of the renewable energy source", Energy Reports Journal, Vol. (8), pp. 11416-11428, Nov. 2022. DOI: [10.1016/j.egy.2022.08.223](https://doi.org/10.1016/j.egy.2022.08.223)